JACS
JOURNAL OF THE AMERICAN CHEMICAL SOCIETY
Communication
pubs.acs.org/JACS

Synthesis of Ethanol via Syngas on Cu/SiO_2 Catalysts with Balanced Cu^0–Cu^+ Sites

Jinlong Gong,[†] Hairong Yue,[†] Yujun Zhao, Shuo Zhao, Li Zhao, Jing Lv, Shengping Wang, and Xinbin Ma*

Key Laboratory for Green Chemical Technology of the Ministry of Education, School of Chemical Engineering and Technology, Tianjin University, Tianjin 300072, China

Supporting Information

ABSTRACT: This paper describes an emerging synthetic route for the production of ethanol (with a yield of ~83%) via syngas using Cu/SiO_2 catalysts. The remarkable stability and efficiency of the catalysts are ascribed to the unique lamellar structure and the cooperative effect between surface Cu^0 and Cu^+ obtained by an ammonia evaporation hydrothermal method. Characterization results indicated that the Cu^0 and Cu^+ were formed during the reduction process, originating from well-dispersed CuO and copper phyllosilicate, respectively. A correlation between the catalytic activity and the Cu^0 and Cu^+ site densities suggested that Cu^0 could be the sole active site and primarily responsible for the activity of the catalyst. Moreover, we have shown that the selectivity for ethanol or ethylene glycol can be tuned simply by regulating the reaction temperature.

Ethanol (EtOH) is a versatile feedstock for the synthesis of various products (e.g., chemicals, fuels, and polymers) and has also been commercially used as an additive or a potential substitute for gasoline.[1] The primary method for EtOH production is based on microbial fermentation processes using agricultural feedstocks, such as sugar cane, potato, manioc, and corn.[2] Conversion of cellulosic materials, although promising,[3] requires considerable R&D effort prior to the achievement of commercial scale.[1] Alternatively, a direct synthesis of EtOH from syngas could complement the existing technologies.[4] However, major disadvantages of this catalytic process include low yields and poor selectivity of EtOH due to slow kinetics of the initial formation of the C–C bond and fast chain growth of the C_2 intermediates.[4a,5]

This paper describes an alternative approach for the synthesis of EtOH via syngas (Scheme 1). This process is an integrated technology consisting of the coupling of CO with methanol to form dimethyl oxalate (DMO) and subsequent hydrogenation to give EtOH. The byproduct of the second step, CH_3OH, can be separated and used in circulation as the feedstock for the coupling step. In fact, the first step has been scaled up into commercial production with a capacity of 10 000 tons per year as of 2010.[6] Thus, this paper focuses on understanding the origin of the high efficiency and stability of Cu-based catalysts for hydrogenation of DMO to EtOH. In particular, the formation of the bifunctional catalytic sites of Cu species (i.e., Cu^+ and Cu^0) and their contribution to the reaction were explored by correlating the surface concentrations of catalyst species with initial rates of reaction.

Scheme 1. Alternative Approach for the Synthesis of EtOH from Syngas

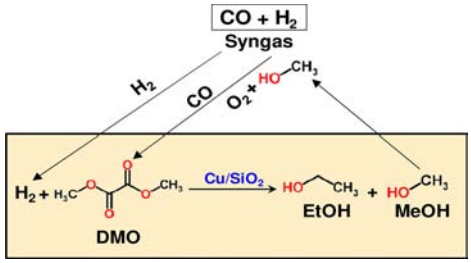

Cu-based catalysts were chosen primarily because of their high activity for vapor-phase hydrogenation reactions.[7] It has been reported that Cu sites account for the selective hydrogenation of C–O bonds and are relatively inactive for the hydrogenolysis of C–C bonds.[7a] Our previous work and the literature on Cu catalysts supported on silica (e.g., SiO_2, hexagonal mesoporous silica, SBA) indicated that high dispersion of copper species and strong metal–support interactions are vital for the high activity and stability in hydrogenation of oxalates to ethylene glycol (EG).[8] In particular, the formation of copper phyllosilicate [$Cu_2SiO_5(OH)_2$] with a lamellar structure can enhance the dispersion and metal–support interactions significantly.[8a,d] Accordingly, we have developed the ammonia evaporation hydrothermal (AEH) method [see the Supporting Information (SI)] to produce catalysts with phyllosilicate phases.

Table 1 illustrates the physicochemical properties and catalytic performance of Cu nanoparticles (NPs) supported on oxides. Al_2O_3 was chosen as a representative acidic oxide support, and ZrO_2 (or TiO_2) and SiO_2 were selected as weakly amphoteric and neutral oxides. Cu/TiO_2, Cu/Al_2O_3, and Cu/ZrO_2 catalysts possess lower activities than the Cu/SiO_2 catalyst, which could be ascribed to the lower Cu dispersions, numbers of surface Cu atoms, and Brunauer–Emmett–Teller (BET) surface areas, as indicated by N_2O titration (Table 1), H_2 temperature-programmed reduction (TPR) (Figure S1 in the SI), and N_2 adsorption, respectively. Indeed, the number of accessible surface Cu atoms was reported to account for the

Received: April 10, 2012
Published: May 24, 2012

 © 2012 American Chemical Society dx.doi.org/10.1021/ja3034153 | J. Am. Chem. Soc. 2012, 134, 13922–13925

Table 1. Physicochemical Properties and Catalytic Performance[a]

entry	catalyst	M loading (%)[b]	yields (%) EtOH	EG	MG	C_3–C_4 diols	Cu dispersion (%)[c]	S_{Cu^0} ($m^2\ g^{-1}$)[c]	S_{Cu^+} ($m^2\ g^{-1}$)[d]	d_M (nm)[e]	S_{BET} ($m^2\ g^{-1}$)	d_{pore} (nm)	V_{pore} ($m^3\ g^{-1}$)
1	8Cu/SiO_2	7.6	28.1	70.7	0	1.2	28.5	15.6	57.8	2.1	285.9	8.1	0.74
2	15Cu/SiO_2	14.7	49.3	35.6	0	15.1	27.3	28.2	76.2	2.7	355.1	8.7	0.93
3	20Cu/SiO_2	19.2	83.0	0	0	17.0	25.8	35.3	72.6	2.8	483.0	9.2	0.89
4	25Cu/SiO_2	23.6	70.7	1.6	0	27.7	20.1	34.7	85.7	4.4	424.5	6.8	0.84
5	30Cu/SiO_2	27.3	58.7	39.8	0	2.3	14.4	26.3	42.2	4.9	389.4	5.9	0.69
6	40Cu/SiO_2	36.8	53.5	34.5	0	12.0	12.7	23.8	28.5	7.8	424.0	5.2	0.72
7	20Cu/SiO_2–IM	19.1	17.9	54.0	21.9	6.2	11.1	15.3	0.5	12.4	283.6	4.7	0.81
8	20Cu/TiO_2	13.4	4.6	39.4	54.7	1.3	2.4	3.3	0.2	26.3	62.1	18.2	0.25
9	20Cu/Al_2O_3	17.2	9.8	61.3	20.7	2.5	5.6	7.6	0.7	10.7	300.1	6.1	0.56
10	20Cu/ZrO_2	14.6	3.3	40.3	52.1	2.0	3.2	4.9	0.3	15.2	54.2	10.2	0.15
11	20Ni/SiO_2[f]	18.3	47.0	0	0	0	–	–	–	8.4	384.4	13.0	1.34
12	20Co/SiO_2[f]	17.6	64.2	0	0	1.8	–	–	–	4.3	378.6	8.9	0.41

[a]Conditions: liquid hour space velocity (LHSV) = 2.0 h^{-1}, H_2/DMO = 200, 553 K. MG: methyl glycolate. C_3–C_4 diols: 1,2-propanediol and 1,2-butanediol. [b]Determined by ICP-AES analysis. M denotes Cu, Ni, or Co. [c]Cu dispersion and surface area of Cu^0 (S_{Cu^0}) were determined by N_2O titration. [d]Surface area of Cu^+ (S_{Cu^+}) was determined from irreversible CO adsorption isotherms. [e]Diameter of metallic particles calculated from the XRD data of the (111) peak broading of Cu by Scherrer equation. [f]Other gaseous products (e.g., CH_4, CO, and CO_2) were also formed.

catalytic hydrogenation performance.[8b] Other nanoclusters (e.g., Ni and Co) supported on silica were also tested: Ni/SiO_2 and Co/SiO_2 were found to be active for the reaction but suffer from a low EtOH selectivity as a result of alcohol decomposition to form CO and subsequent methanation of CO to form methane.[9] Notably, neutral SiO_2-supported Cu catalysts prepared by the AEH method exhibited better activity than those prepared by conventional impregnation.

To understand the origin of the catalytic reactivity over Cu/SiO_2 catalysts, we further investigated the catalytic performance for the gas-phase hydrogenation of DMO by tuning the Cu loading. Table 1 shows that the 20% Cu/SiO_2 (20Cu/SiO_2) catalyst exhibited superior catalytic reactivity in comparison with the others. Figure 1 presents the performance of the 20Cu/SiO_2 catalyst for hydrogenation of DMO as a function of reaction temperature (453–573 K) and the results of a stability test at 553 K for 200 h. Remarkably, the DMO conversion remained at 100% at temperatures above 473 K, and the selectivity for EtOH increased with increasing temperature, exceeding 80% at 553 K. One interesting feature is that formation of EG is favorable at temperatures lower than 553 K, whereas elevated temperatures (e.g., above 553 K) induce the intermolecular dehydrogenation of EtOH and methanol with EG to form C_3–C_4 diols,[8a] which diminishes the selectivity for EtOH. The catalyst was quite stable at 553 K, with constant conversion of DMO (100%) and selectivity for EtOH (~83%). Transmission electron microscopy (TEM) and powder X-ray diffraction (PXRD) results for the reduced and used samples (Figures S2 and S3) provide basic clues concerning the high activity and stability of the catalysts . The Cu species was not sintered in a 200 h test, indicating that the unique structure of phyllosilicate hampers the sintering of the Cu NPs. In addition, the change in content of surface Cu and the chemical environment was nearly negligible as determined by X-ray photoelectron spectroscopy (XPS) (Figure 2 and Table S1 in the SI). The excellent stability lies in the formation of copper phyllosilicates, as confirmed by the lamellar structure in the TEM image of the calcined 20CuSiO$_2$ catalyst (Figure 3A). The structure could stem from its unique preparation method; it is formed via reaction of the Cu^{2+} complex with the silanol groups

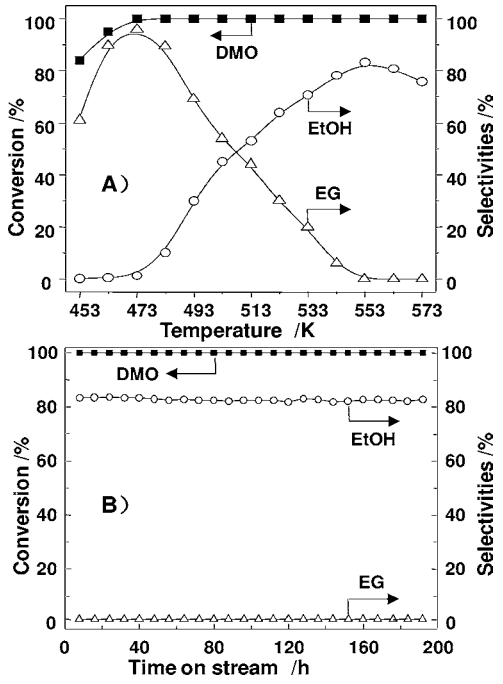

Figure 1. Performance of the 20Cu/SiO_2 catalyst in catalytic hydrogenation of DMO. (A) DMO conversion and product selectivities as functions of reaction temperature (453–573 K). (B) DMO conversion and EtOH selectivity vs time on stream at 553 K. Reaction conditions: liquid hour space velocity (LHSV) = 2.0 h^{-1}, H_2/DMO = 200 (mol/mol). Trace byproducts include MG and C_3–C_4 diols.

of the silica surface via hydrolytic adsorption to form ≡SiOCu^{II} monomer and subsequent further polymerization.[8a,b,10] Because of the strong interaction between the metal and SiO_2, this complex could supply stable Cu species on the surface that would remain intact even after our experimental calcination, reduction, and reaction.

We hypothesize that the high catalytic activity for hydrogenation of DMO to EtOH results from a cooperative effect between Cu^0 and Cu^+. To understand the structure of the Cu

dx.doi.org/10.1021/ja3034153 | J. Am. Chem. Soc. 2012, 134, 13922–13925

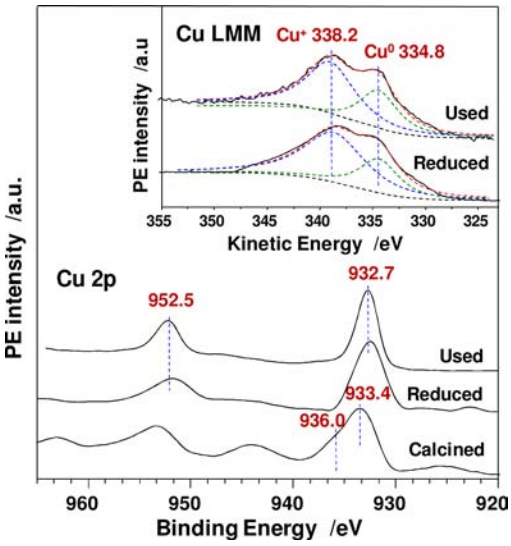

Figure 2. Cu 2p XPS spectra and (inset) Cu LMM XAES spectra of calcined, reduced, and used 20Cu/SiO_2 samples.

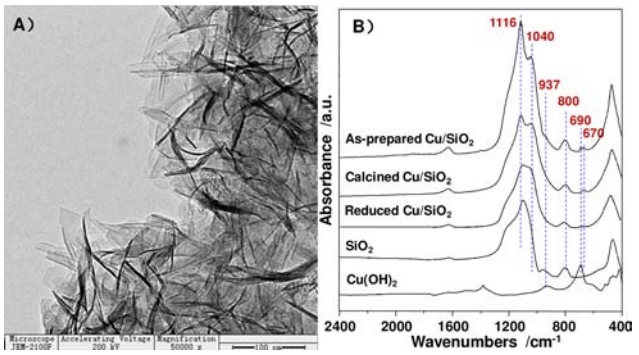

Figure 3. (A) TEM image of the calcined 20CuSiO_2 catalyst. (B) FTIR spectra of as-prepared, calcined, and reduced 20Cu/SiO_2, SiO_2, and pure $Cu(OH)_2$ samples.

species and the formation process leading to the coexistence of Cu^0 and Cu^+ in our Cu/SiO_2 catalysts prepared by the AEH method, we characterized the Cu species in the synthetic process. Fourier-transform IR (FTIR) spectroscopy was used to discriminate the copper hydroxide and copper phyllosilicate species.[10b,11] Because of their structural OH groups, the frequencies of the δ_{OH} bands for copper hydroxide are at 938 and 690 cm^{-1},[11] while those for copper phyllosilicate are at 1040 and 670 cm^{-1}.[8a,10b] For the as-prepared 20Cu/SiO_2 catalyst (Figure 3B), the peaks appearing at 690 and 937 cm^{-1} suggest the presence of $Cu(OH)_2$. This was also confirmed by the diffraction peaks for $Cu(OH)_2$ species (JCPDS no. 13-0420) in the PXRD pattern (Figure S3). The appearance of the δ_{OH} vibration at 670 cm^{-1} and the ν_{SiO} shoulder peak at 1040 cm^{-1} indicated that the structure of copper phyllosilicate existed in the samples; these were not seen for the 20Cu/SiO_2–IM sample prepared by the impregnation method (Figure S4). Upon calcination, the absorption bands associated with $Cu(OH)_2$ disappeared, indicating the complete decomposition of $Cu(OH)_2$ to CuO. However, the presence of the δ_{OH} vibration at 670 cm^{-1} in the calcined 20Cu/SiO_2 sample suggests the existence of the structure of copper phyllosilicate even after calcination at 673 K. The XPS data for the calcined samples (Figure 2) shows that the Cu oxidation state is +2 with a d^9 electron configuration in the calcined sample, as evidenced by the Cu $2p_{3/2}$ peak at ~933.3 eV, the Cu $2p_{1/2}$ peak at ~952.5 eV, and the 2p → 3d satellite peak between 942 and 944 eV.[8a] The asymmetry of the Cu $2p_{3/2}$ envelope allowed the peak of the calcined sample to be deconvoluted into two contributions entered around 933.4 and 936.0 eV, corresponding to dispersed CuO and copper phyllosilicate, respectively.[12]

The formation of Cu^+ and Cu^0 occurs during the reduction process, as indicated by the disappearance of the Cu 2p satellite peak at 942–944 eV in the XPS spectrum and the appearance of two overlapping peaks at 334.8 and 338.2 eV in the Cu LMM X-ray excited Auger spectroscopy (XAES) spectrum for the sample after reduction (Figure 2).[8b] The distinguishability was also confirmed via diffraction peaks in the PXRD patterns (Figure S3). Strong diffraction peaks of the reduced catalysts at 35.8° are ascribable to the $Cu_2O(111)$ plane (JCPDS no. 05-0667), while the diffraction peaks at 43.3, 50.4, and 74.1° are characteristic of Cu^0 (JCPDS no. 04-0836). The Cu^+ species is formed upon the reduction of the copper phyllosilicate under the experimental conditions (e.g., 623 K), since the further reduction of Cu^+ to Cu^0 requires a temperature higher than 873 K.[8a] Since the reduction of CuO to Cu^0 occurs at ~510 K,[13] the single TPR peak at ~516 K (Figure S1) could be attributed to the collective contribution of the stepwise reduction of the well-dispersed CuO to Cu^0 and copper phyllosilicate to Cu^+.[13,14]

To further gain insight into the effect of the Cu valence state on the hydrogenation of DMO to EtOH, we examined the effect of Cu loading on the EtOH yield and turnover frequency (TOF) of EtOH as a function of $Cu^0/(Cu^0 + Cu^+)$ (Figure 4).

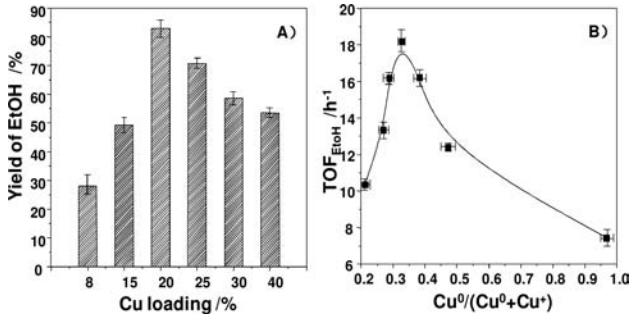

Figure 4. (A) Yield of EtOH as a function of Cu loading. (B) Correlation of the TOF of EtOH with $Cu^0/(Cu^0 + Cu^+)$.

It is notable that the TOF of EtOH increased steadily at low $Cu^0/(Cu^0 + Cu^+)$, reached a maximum at $Cu^0/(Cu^0 + Cu^+)$ = 0.33, and decreased with further increases in the ratio (Figure 4B). Therefore, the optimal TOF of EtOH on the 20Cu/SiO_2 catalyst lies in the high surface Cu^0 site density (Table 1) and the cooperative effect of Cu^0 and Cu^+. Moreover, the strong correlation between the surface Cu^0 site density and the formation rates of EtOH and C_3–C_4 diols and the intercept of the trend line (Figure S5A) suggest that the catalytic activity depends on the number of Cu^0 sites. In comparison, there is no clear correlation between the specific activity and the number of Cu^+ sites (Figure S5B).

Two general mechanisms were accordingly proposed and tested on the basis of our experimental results indicating a synergetic effect. In the first, the catalyst has only one active site, Cu^0, on which H_2 is activated, and the reactant is adsorbed through the hydroxyl group and cleaved. The second is a two-site mechanism in which the Cu^0 species activates H_2 and the

dx.doi.org/10.1021/ja3034153 | J. Am. Chem. Soc. 2012, 134, 13922–13925

Cu^+ species adsorbs the carbonyl group.[15] The correlation in Figure 4 and Figure S5 indicates that Cu^0 is the active site but cannot rule out the role of Cu^+ in a two-site mechanism. However, it has been suggested that in methyl acetate hydrogenation, Cu^+ acts as the stabilizer of the methoxy and acyl species, which are intermediates in DMO hydrogenation.[15] In addition, Cu^+ sites could function as electrophilic or Lewis acidic sites to polarize the C═O bond via the electron lone pair in oxygen, thus improving the reactivity of the ester group in DMO.[8b] Therefore, it is very likely that Cu^0 acts as the primary active site, which is consistent with the hydrogenation of dimethyl maleate,[16] diethyl oxalate,[17] and furfural and crotonaldehyde,[18] while the Cu^+ species facilitates conversion of intermediates.

Another interesting feature is the tunability of the products as a function of reaction temperature (Figure 1). For example, a high yield (ca. 95%) of EG can be obtained at a lower temperature (e.g., 473 K). EG is an important chemical used in a variety of industrial applications, such as antifreeze, polyester, H_2 energy, and fuel cells.[19] At present, the technology of ethylene oxidation/hydration accounts for the major share of the EG market.[20] As ethylene oxide is commercially produced from ethylene via petroleum cracking, and the global market demand for EG always surpasses its production capacity, increasing efforts have been devoted to exploring alternative processes.[21] Therefore, this emerging synthetic route for the main production of EtOH or EG from syngas using the same catalytic system through control of the temperature (Scheme S1) could become considerably significant and promising in industry.

In summary, we have demonstrated a facile and highly efficient route for the synthesis of EtOH using low-cost Cu/SiO_2 catalysts prepared by the AEH method. The catalysts possess remarkable stability and efficiency, which could be ascribed to the coexistence of Cu^0 and Cu^+ primarily originating from well-dispersed CuO NPs and copper phyllosilicate, respectively. The correlation between the activity and the Cu^0 and Cu^+ site densities suggests that Cu^0 is the active site and primarily responsible for the activity of the catalyst, while Cu^+ facilitates the conversion of intermediates. Moreover, the selectivity for EtOH and EG can be tuned simply by regulating the reaction temperature. This indirect synthetic methodology using inexpensive Cu-based catalysts under facile conditions is a promising process that has the potential to enable a sustainable EtOH and EG synthesis using syngas from practical point of view.

■ ASSOCIATED CONTENT

Ⓢ Supporting Information

Details of experimental procedures, catalyst characterization, TPR profiles, TEM images, PXRD patterns, XPS and FT-IR spectra, and correlation of formation rate with the Cu^0 and Cu^+ surface areas. This material is available free of charge via the Internet at http://pubs.acs.org.

■ AUTHOR INFORMATION

Corresponding Author

xbma@tju.edu.cn

Author Contributions

†J.G. and H.Y. contributed equally.

Notes

The authors declare no competing financial interest.

■ ACKNOWLEDGMENTS

This research was supported by the Program for New Century Excellent Talents in University (NCET-10-0611), the China Postdoctoral Science Foundation (20090450090), the Seed Foundation of Tianjin University (60303002), and the Program of Introducing Talents of Discipline to Universities (B06006).

■ REFERENCES

(1) Goldemberg, J. *Science* **2007**, *315*, 808.
(2) (a) Cleveland, C. J.; Hall, C. A. S.; Herendeen, R. A. *Science* **2006**, *312*, 1746. (b) Ragauskas, A. J.; Williams, C. K.; Davison, B. H.; Britovsek, G.; Cairney, J.; Eckert, C. A.; Frederick, W. J.; Hallett, J. P.; Leak, D. J.; Liotta, C. L.; Mielenz, J. R.; Murphy, R.; Templer, R.; Tschaplinski, T. *Science* **2006**, *311*, 484.
(3) Farrell, A. E.; Plevin, R. J.; Turner, B. T.; Jones, A. D.; O'Hare, M.; Kammen, D. M. *Science* **2006**, *311*, 506.
(4) (a) Choi, Y.; Liu, P. *J. Am. Chem. Soc.* **2009**, *131*, 13054. (b) Spivey, J. J.; Egbebi, A. *Chem. Soc. Rev.* **2007**, *36*, 1514. (c) Haider, M. A.; Gogate, M. R.; Davis, R. J. *J. Catal.* **2009**, *261*, 9. (d) Pan, X.; Fan, Z.; Chen, W.; Ding, Y.; Luo, H.; Bao, X. *Nat. Mater.* **2007**, *6*, 507.
(5) Subramani, V.; Gangwal, S. K. *Energy Fuels* **2008**, *22*, 814.
(6) (a) Gao, X.; Zhao, Y.; Wang, S.; Yin, Y.; Wang, B.; Ma, X. *Chem. Eng. Sci.* **2011**, *66*, 3513. (b) Gao, Z.; Liu, Z.; He, F.; Xu, G. *J. Mol. Catal. A: Chem.* **2005**, *235*, 143.
(7) (a) Brands, D. S.; Poels, E. K.; Bliek, A. *Appl. Catal., A* **1999**, *184*, 279. (b) Sodesawa, T.; Nagacho, M.; Onodera, A.; Nozaki, F. *J. Catal.* **1986**, *102*, 460. (c) Kobayashi, H.; Takezawa, N.; Minochi, C. *J. Catal.* **1981**, *69*, 487.
(8) (a) Chen, L. F.; Guo, P. J.; Qiao, M. H.; Yan, S. R.; Li, H. X.; Shen, W.; Xu, H. L.; Fan, K. N. *J. Catal.* **2008**, *257*, 172. (b) Yin, A. Y.; Guo, X. Y.; Dai, W. L.; Fan, K. N. *J. Phys. Chem. C* **2009**, *113*, 11003. (c) Guo, X. Y.; Yin, A. Y.; Dai, W. L.; Fan, K. N. *Catal. Lett.* **2009**, *132*, 22. (d) Yue, H.; Zhao, Y.; Zhao, L.; Lv, J.; Wang, S.; Gong, J.; Ma, X. *AIChE J.* **2012**, DOI: 10.1002/aic.12785.
(9) Huber, G. W.; Shabaker, J. W.; Dumesic, J. A. *Science* **2003**, *300*, 2075.
(10) (a) Burattin, P.; Che, M.; Louis, C. *J. Phys. Chem. B* **1998**, *102*, 2722. (b) Toupance, T.; Kermarec, M.; Lambert, J.-F.; Louis, C. *J. Phys. Chem. B* **2002**, *106*, 2277.
(11) Huang, Z.; Cui, F.; Xue, J.; Zuo, J.; Chen, J.; Xia, C. *J. Phys. Chem. C* **2010**, *114*, 16104.
(12) Gervasini, A.; Manzoli, M.; Martra, G.; Ponti, A.; Ravasio, N.; Sordelli, L.; Zaccheria, F. *J. Phys. Chem. B* **2006**, *110*, 7851.
(13) Marchi, A. J.; Fierro, J. L. G.; Santamaría, J.; Monzón, A. *Appl. Catal., A* **1996**, *142*, 375.
(14) Van Der Grift, C. J. G.; Muldera, A.; Geusa, J. W. *Appl. Catal.* **1990**, *60*, 181.
(15) Poels, E. K.; Brands, D. S. *Appl. Catal., A* **2000**, *191*, 83.
(16) Mokhtar, M.; Ohlinger, C.; Schlander, J. H.; Turek, T. *Chem. Eng. Technol.* **2001**, *24*, 423.
(17) Xu, G.; Li, Y.; Li, Z.; Wang, H. *Ind. Eng. Chem. Res.* **1995**, *34*, 2371.
(18) Dandekar, A.; Baker, R. T. K.; Vannice, M. A. *J. Catal.* **1999**, *184*, 421.
(19) (a) Celik, F. E.; Kim, T.; Bell, A. T. *Angew. Chem.* **2009**, *121*, 4907. (b) Cortright, R. D.; Davda, R. R.; Dumesic, J. A. *Nature* **2002**, *418*, 964. (c) Bianchini, C.; Shen, P. K. *Chem. Rev.* **2009**, *109*, 4183.
(20) (a) Yin, A. Y.; Guo, X. Y.; Dai, W. L.; Fan, K. N. *Chem. Commun.* **2010**, *46*, 4348. (b) Lin, J.; Zhao, X.; Cui, Y.; Zhang, H.; Liao, D. *Chem. Commun.* **2012**, *48*, 1177.
(21) Yue, H.; Zhao, Y.; Ma, X.; Gong, J. *Chem. Soc. Rev.* **2012**, *41*, 4218.